Multi-decadal Validation of the TIMELINE AVHRR Land Suface Temperature Product with MODIS and in situ LST

Philipp Reiners
Deutsches Fernerkundungsdatenzentrum (DFD)
Deutsches Zentrum für Luft- und Raumfahrt (DLR)

At LST CCI User Workshop 2020

By Patrick Chappatte, Source: www.climatechangenews.com

How can we make Global Warming visible?

AVHRR – Long-term EO Data with daily Resolution

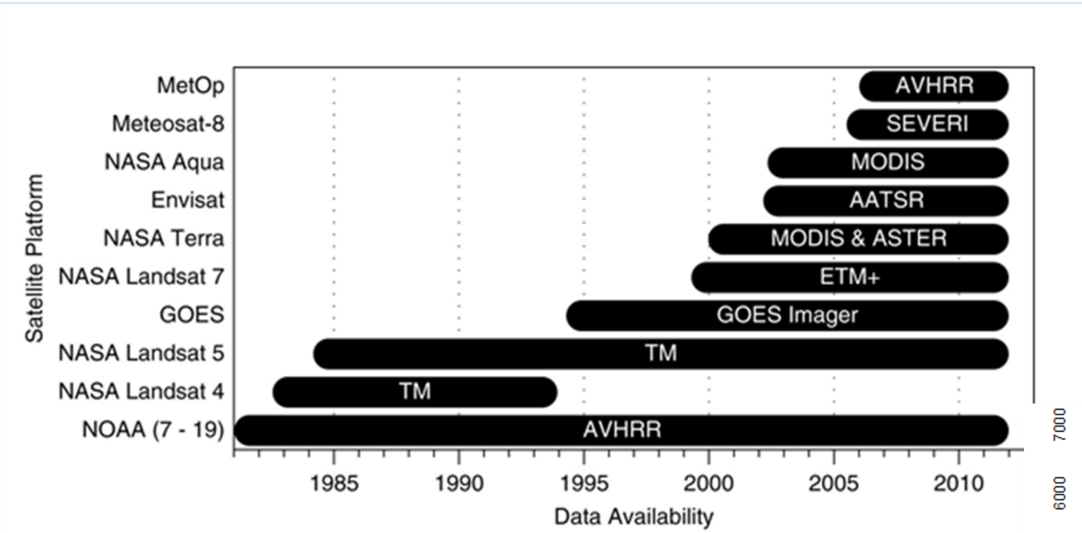

Fig. 1: Timeline of data availability taken from Tomlinson et al. (2011)

- Long remote sensing time series with high accuracy
- AVHRR: 40 years long time series, daily repeat, 1 km resolution

- 150 000 AVHRR LAC scenes received and stored at DFD
- Scenes from 10 different NOAA satellites, AVHRR/1 , 2 and 3

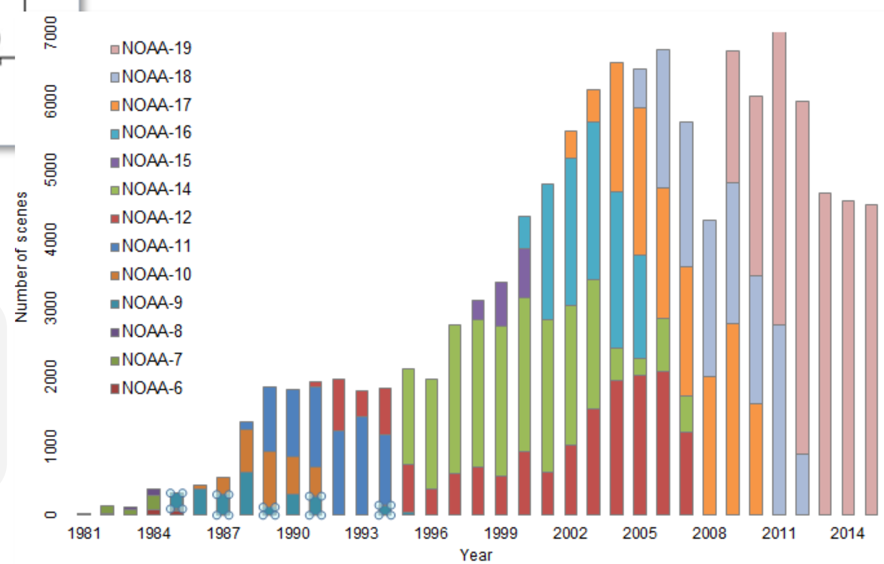

Fig. 2: AVHRR LAC scenes at DFD taken from the TIMELINE project site

The TIMELINE Project

- Consistent time series from AVHRR over Europe and Africa
- Level 0: AVHRR scenes in HRPT format
- Level 1B: TOA Reflectance/Temperature
- Level 2 : Environmental variables in orbit projection
- Level 3: daily, 10-day and monthly composites in geographic projection

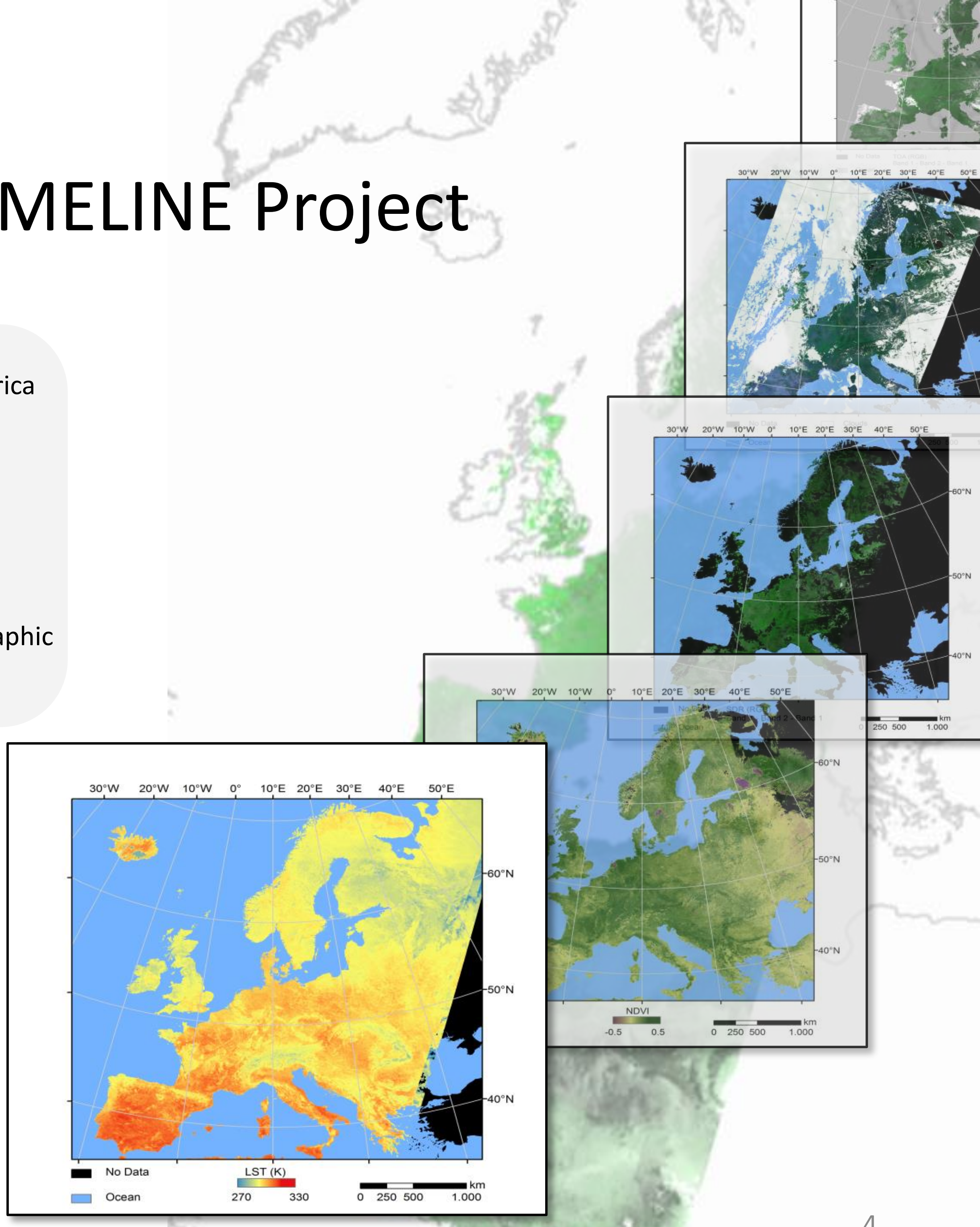

L0 L1B L2

The TIMELINE LST Framework

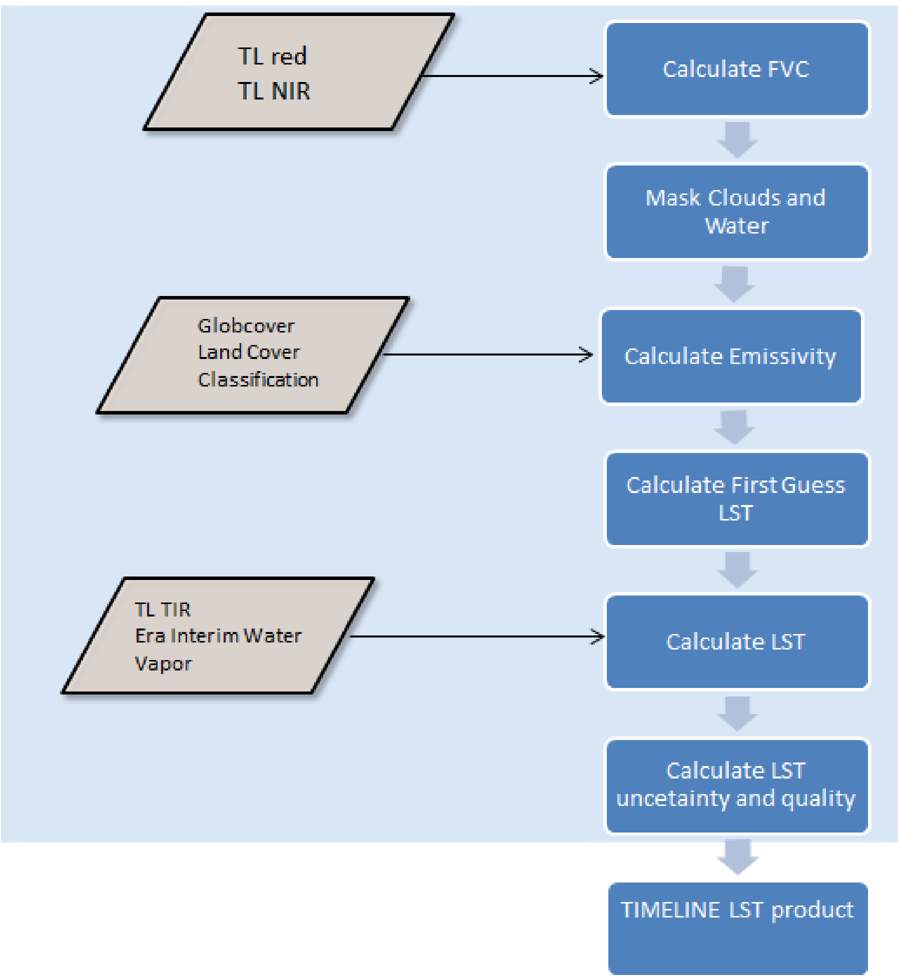

Vegetation Cover Method by Caselles et al (2012)

$$\varepsilon_k = \varepsilon_{kv}\ f + \varepsilon_{kg}\ (1-f) + 4 < d\varepsilon_k > f\ (1-f)$$

Split window algorithm by Becker & Li (1990)

$$\alpha = 1 + p_1 \frac{1-\varepsilon}{\varepsilon} + p_2 \frac{d\epsilon}{\varepsilon^2}$$

$$\beta = p_3 + p_4 \frac{1-\varepsilon}{\varepsilon} + p_5 \frac{d\epsilon}{\varepsilon^2}$$

$$LST = p_0 + \alpha\left(\frac{t4+t5}{2}\right) + \beta\left(\frac{t4-t5}{2}\right)$$

Mono window algorithm by Qin et al (2001)

$$LST = \frac{1}{c}(p_2(1-c-d) + t_3(p_1(1-c-d)+c+d) - dT_{atm})$$

$$c = \varepsilon_4 \tau$$

$$d = (1-\tau)(1+\tau(1-\varepsilon_4))$$

$$\tau = p_0 - p_1 cwv$$

Fig. 3: Emissivity and LST algorithms taken from Frey et al. (2017)

The coefficients p0-p5 minimize the effects of sensor characteristics, LST range, TCWV and sensor view angle. They were derived running MODTRAN 5.3 on atmospheric profiles from Seebor 5.0.

Validation Sites

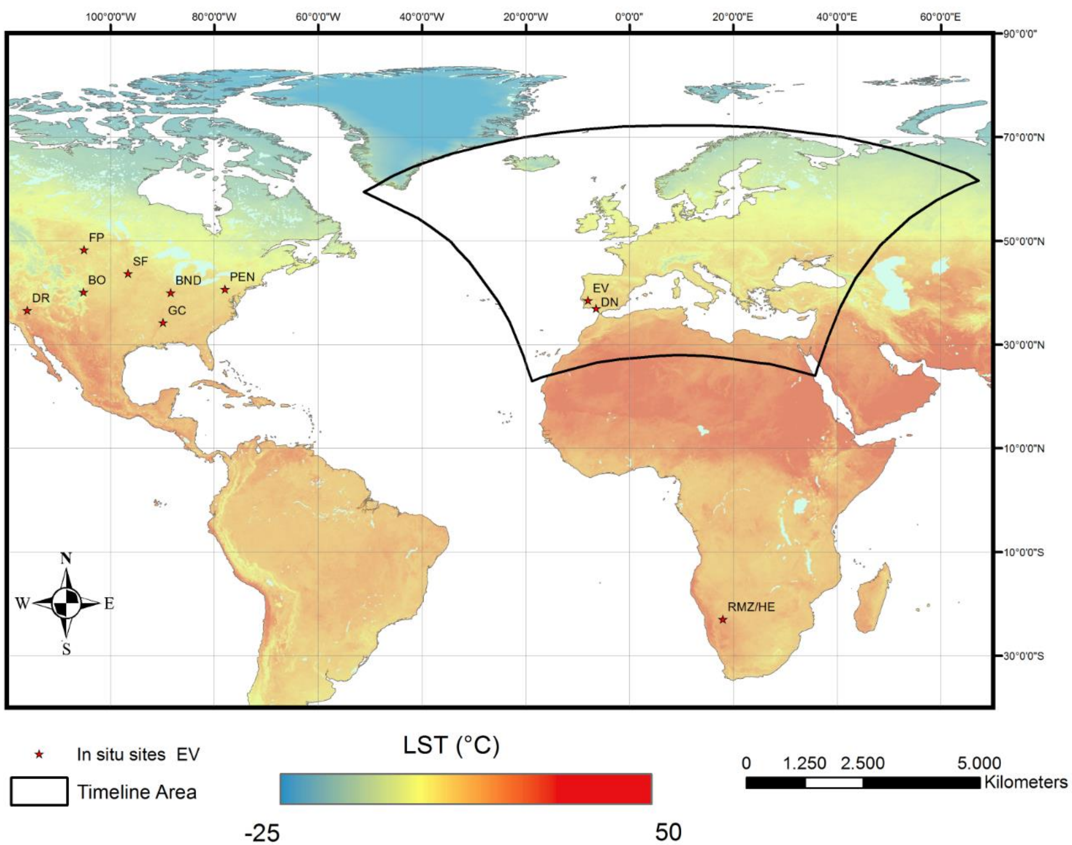

Fig. 4: Map of in situ sites, Reiners et al. , in preparation of publication

Station	Lat	Lon	Landcover
Bondville	40	-88.3	Grassland
Boulder	40.1	-105.2	Grassland
Desert Rock	36.6	-116	Shrubland
Fort Peck	48.3	-105.1	Grassland
Goodwin Creek	34.2	-89.8	Grassland
Pennsylvania State Univ.	40.7	-77.9	Cropland
Sioux Falls	43.7	-96.6	Grassland
Heimat	-22.9	18	Grassland
Donana	37	-6.4	Grassland
Evora	38.5	-8	Grassland

DLR

TIMELINE

Results of the in situ Validation

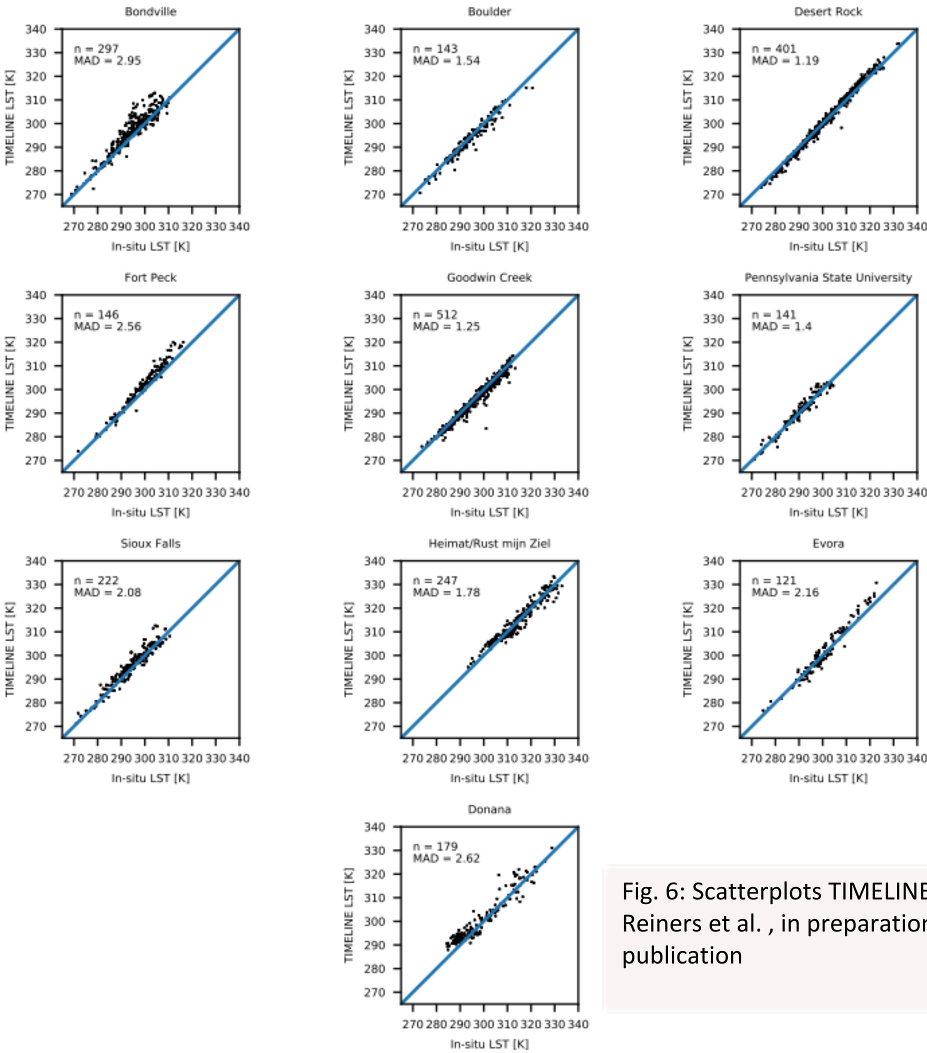

Fig. 6: Scatterplots TIMELINE/in situ LST, Reiners et al. , in preparation of publication

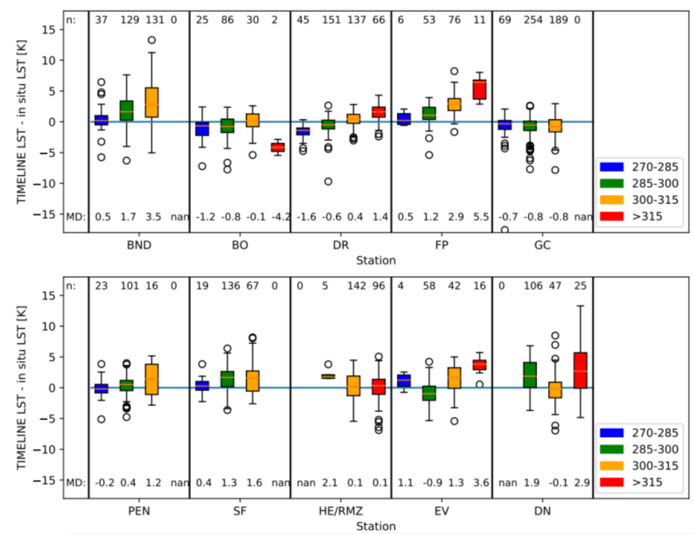

Fig. 5: Boxplots TIMELINE – in situ LST for LST ranges, Reiners et al. , in preparation of publication

- The in situ validation was conducted for the years 2010-2013
- In total, 2409 individual in situ measurements were compared to the TIMELINE LST
- The comparison resulted in MADs between 1.24 K and 2.96 K and RMSEs between 1.61 K and 3.97 K
- On average, an absolute deviation of 1.83 K was observed
- The deviation strongly depends on the LST range and lightly depends on the sensor view and sun zenith angle. TCWV did not cause any impact.

Results of the Comparison with MODIS LST

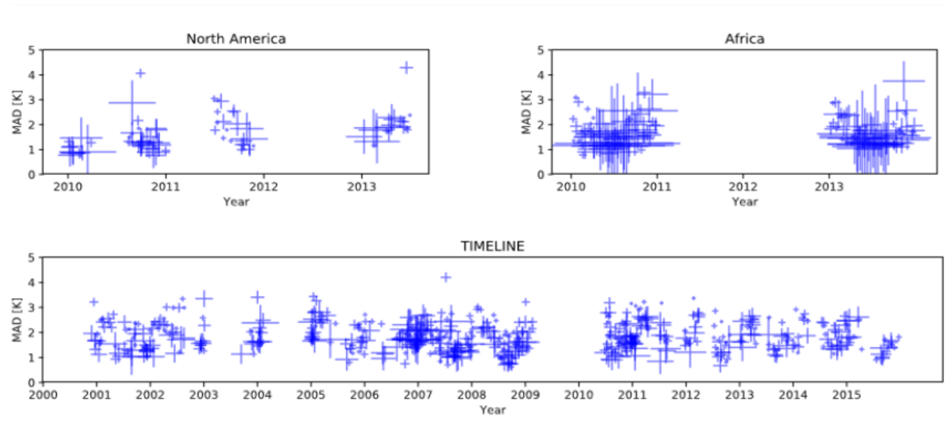

- 574 TIMELINE/MOD11_L2 LST scenes over Europe, 77 over North America and 123 over Africa were analyzed
- The comparison showed a high seasonal variance with MADs between 1 and 2 K in the winter months and 2 and 3 K in the summer months. An average deviation of 1.4 K was observed

Fig. 7: MAD between TIMELINE and MODIS LST per TIMELINE/MODIS scene, Reiners et al. , in preparation of publication

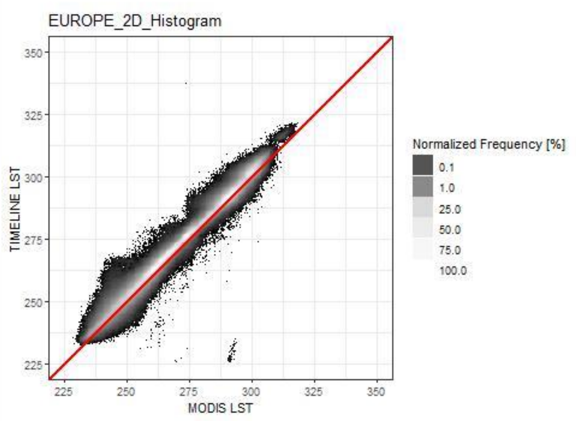

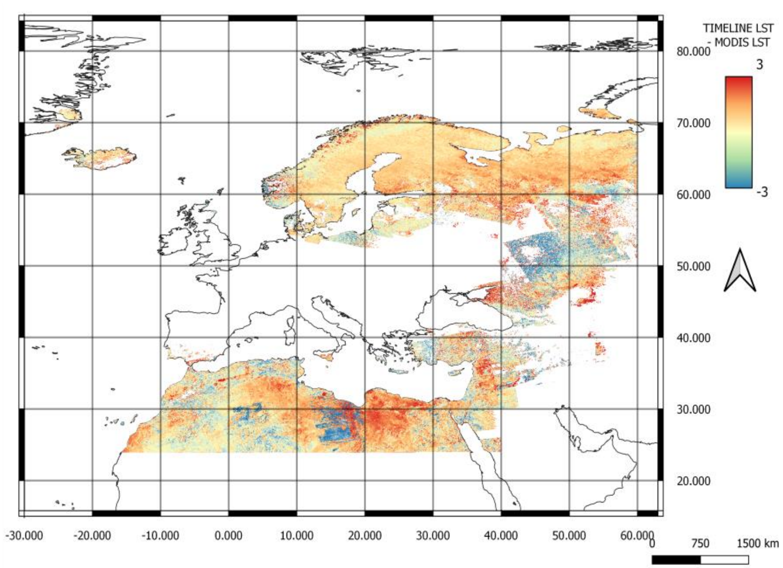

- Positive bias of TIMELINE LST towards MODIS LST became visible, especially at high LST ranges

Fig. 8: Density scatterplot of all TIMELINE/MODIS observations over Europe, Reiners et al. , in preparation of publication

Fig. 9: Average difference between TIMELINE and MODIS LST of all TIMELINE/MODIS observations over Europe, Reiners et al. , in preparation of publication

TIMELINE LST Time Series

L2 LST Abisko/Schweden (68.35°N/18.817°E, Wald)

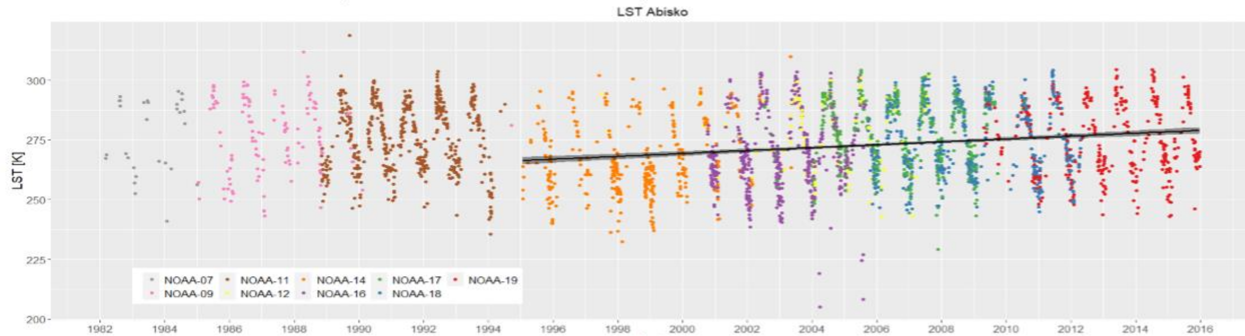

First time series analysis indicates a satisfactory consistency of the TIMELINE product, as no offsets across-sensors could be detected.

Fig. 10:TIMELINE LST at Abisko, Sweden, Reiners et al. , in preparation of publication

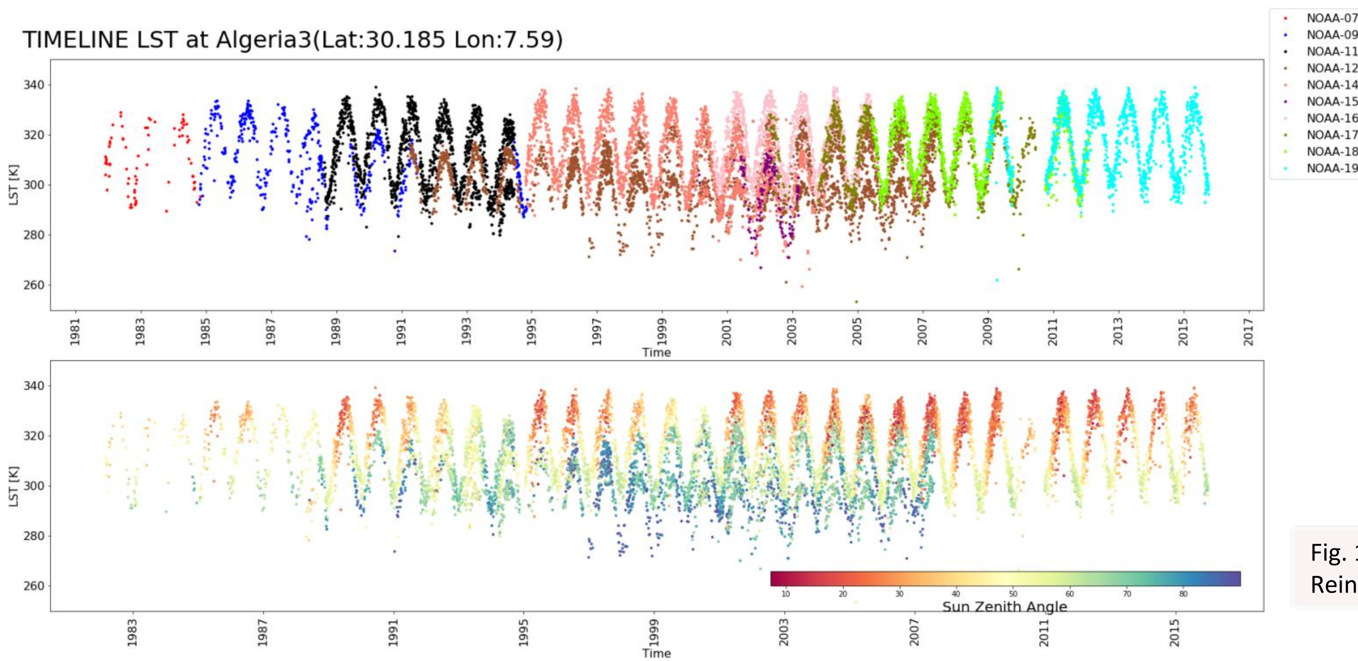

Problem: The satellites have different overpass times and experience orbit drift.

➡ Daytime normalization is necessary to analyze the full TIMELINE LST time series.

Fig. 11: TIMELINE LST at Algeria3, Algeria, Reiners et al. , in preparation of publication

Conclusions and Outlook

- The validation with in situ LST resulted in MADs between 1.24 K and 2.96, which is in the accuracy range of other LST studies
- The comparison with MODIS LST showed a positive bias of TIMELINE LST
- First time series analysis shows consistency across sensors
- Further validation including in situ sites with different land cover is necessary
- Modelling the diurnal LST cycle is necessary to derive long term trends for whole Europe

- Modell spatially and temporally continuous LST for Europe and North Africa
- Develope Level 3 daily, 10-day and monthly composites
- Develope large-area and long-term environmental models using the TIMELINE products in combination with other EO data
- Adapt TIMELINE LST framework to derive SST

Create the foundation for multi-decadal and climate-relevant statements for decision makers, the scientific community, the UN and NGOs!

References

Becker, F.; Li, Z.-L. Towards a local split window method over land surfaces. *International Journal of Remote Sensing* **1990**, *11*, 369–393.

Caselles, E.; Valor, E.; Abad, F.; Caselles, V. Automatic classification-based generation of thermal infrared land surface emissivity maps using AATSR data over Europe. *Remote Sensing of Environment* **2012**, *124*, 321–333.

Frey, C.M.; Kuenzer, C.; Dech, S. Assessment of Mono- and Split-Window Approaches for Time Series Processing of LST from AVHRR - A TIMELINE Round Robin. *Remote Sensing* **2017**, *9*.

Göttsche, F.-M.; Olesen, F.-S.; Trigo, I.F.; Bork-Unkelbach, A.; Martin, M.A. Long Term Validation of Land Surface Temperature Retrieved from MSG/SEVIRI with Continuous in-Situ Measurements in Africa. *Remote Sensing* **2016**, *8*.

Qin, Z.; Karnieli, A.; Berliner, P. A mono-window algorithm for retrieving land surface temperature from Landsat TM data and its application to the Israel-Egypt border region. *International Journal of Remote Sensing* **2001**, *22*, 3719–3746.

Skokovic, D.; Sobrino, J.A.; Jimenez-Munoz, J.C.: Vicarious Calibration of the Landsat 7 Thermal Infrared Band and LST Algorithm Validation of the ETM+ Instrument Using Three Global Atmospheric Profiles. *Transaction on Geoscience and Remote Sensing, Vol. 55, No. 3*, **2017**

Tomlinson, C.J.; Chapman, L.; Thornes, J.E.; Baker, C. Remote sensing land surface temperature for meteorology and climatology: a review. *Meteorological Applications* **2011**, *18*, 296–306.